

Nonlinear model predictive control-based active power dispatch strategy for wind power plant considering dynamic wake effect

Zhengyang Hu, Bingtuan Gao*, Yongheng Mao

School of Electrical Engineering, Southeast University, Nanjing, China



ARTICLE INFO

Keywords:

Wind power plant
Active power dispatch
Model predictive control
Wake effect
Active power support capability

ABSTRACT

Inappropriate active power dispatch strategies can diminish the active power support capability (APSC) of the wind power plant (WPP) due to the wake effect. In existing strategies, the WPP's APSC and the time delay of wake effect are not thoroughly investigated. This paper proposes an active power dispatch strategy to increase the WPP's APSC while tracking the power reference. First, WPP's temporary and sustained APSCs are analyzed considering dynamic wake effect. Correspondingly, the total stored kinetic energy and increasable power of WPP are introduced as evaluation indicators of the capabilities. Furthermore, a bi-level control framework is proposed to accomplish the dispatch task in different timescales. Aiming at improving WPP's temporary and sustained APSCs comprehensively, the operating status references of each WT, including the power reference and pitch angle, are optimized in the WPP layer. Taking the time delay and nonlinearity of wake effect into account, the receding horizon optimization is solved in a finite time domain using nonlinear model predictive control (NMPC). During the sampling interval of the NMPC, a coordinated control in the WT layer is developed to modify the active power reference dispatched by the WPP layer in case the wind speed fluctuates. Finally, extensive case studies show that the WPP's temporary and sustained APSCs are improved with the proposed strategy in different wind conditions and power references.

1. Introduction

Wind power generation has grown quickly in recent years as one of the most promising techniques for alleviating energy shortages and addressing high carbon emission challenges [1,2,3]. Integrating wind power in modern power system will reduce dependency on fossil fuels. However, the high penetration of wind power based on the maximum power point tracking (MPPT) method may produce a supply–demand imbalance in power system due to the intermit and stochastic character of wind sources [4]. Accordingly, more challenges rise to the power system frequency stability. To address this issue, wind power plants (WPPs) should track the power instruction from the system operator and possess the ability to participate in frequency regulation at the same time.

Energy storage systems can reduce WPP's influence on system frequency stability, but excessive investment has to be involved [5]. As a result, the active power support capability (APSC) of the WPP should be fully utilized preferentially. Considering the uncertainties of wind sources and load power, active power regulation strategy, including

deloading and overloading, should be implemented in a WPP [6]. Furthermore, according to the risk assessment of power system, WPPs are expected to function as the reserved power sources in the event of possible power system faults. Consequently, the active power reserve of a WPP is essential for system integration, and the power curtailment technique of a WPP has become an inevitable choice for providing necessary frequency support rather than the cost-effective MPPT scheme [7].

The rotor speed control (RSC) and pitch angle control (PAC) are the two major approaches for achieving active power regulation of wind turbines (WTs) [8]. In [9], the RSC is adopted in the deloading operation by shifting the MPPT curve to the right-side suboptimal curve. In addition, the coordinated PAC is presented to prevent the rotor speed from exceeding the limit [10], so that the acquired wind energy of WTs can be regulated in both low and high wind speed conditions. A load sharing control scheme for a WPP with the same deloading rate is proposed in [11]. However, the differences of the WTs' operating conditions caused by the wake effect are nonnegligible [12]. Taking wake effect into consideration, most research focuses on the maximization of

* Corresponding author.

E-mail address: gaobingtuan@seu.edu.cn (B. Gao).

the kinetic energy stored in WTs. A load sharing control technique with variable deloading coefficient is proposed in [13]. The rate of power curtailment (ROPC) of each WT is proportional to the difference between the current rotor speed and its upper limit. As a result, the ROPC of downstream WTs, whose rotor speeds are relatively lower, are larger than that of upstream WTs, raising the priority of RSC especially for the downstream WTs. The distributed deloading control of WPP for load sharing is investigated in [14], also aiming at improving the priority of RSC. For a single WT, increasing the stored kinetic energy can improve the temporary APSC and reduce wind energy losses, but it is not the case from the perspective of WPP.

The purpose of the control of WPP is to coordinate each WT to obtain integral external characteristics. The time-lapse wake effect and the output characteristics of WTs result in the two difficulties in the control of WPP, which are the time delay and nonlinearity. Few studies have paid attention to the time delay of the wake effect from upstream to downstream. As a result, the significant time delay of the influence of the upstream WT on the downstream WT is ignored. As for the nonlinearity, an optimization method is proposed in [15] to maximize the output active power of the WPP. [16] proposes a frequency control scheme for WPP by optimizing the operating status of WTs to maximize the captured wind energy as well as the stored kinetic energy. However, the neglect of the time delay reduces the reliability of optimization results. The characteristics of the thrust coefficient of WT versus rotor speed and pitch angle have a strong nonlinearity. Accordingly, the RSC and PAC have effects on wake effect, and then affect the potential output capability of the whole WPP. The power dispatch strategy for WPP and the regulation priority of each row of WT under the influence of the wake effect are studied in [17] considering that overspeed will further aggravate the wake effect. The sequence of RSC and PAC actions for each row of wind turbines has been adjusted, and the RSC still has a higher priority than PAC. However, such a high priority of RSC may not be an optimal choice in terms of the output characteristics of WPP during the electro-mechanical transient timescale.

Taking the time delay and nonlinearity of the wake effect into account, the active power dispatch of WPP can be transformed into a receding horizon optimization problem in a finite time domain. Model predictive control (MPC) can be an appropriate control method to deal with such a problem. Since MPC is skilled in dealing with constrained optimization problems and taking advantage of predictive information, it has been used in the active power control and dispatch of WPP in recent years. A bi-level model predictive control strategy based on dynamic active power dispatch is proposed in [18,19], but the wake effect is ignored. An active power control strategy for WPP considering fatigue loads of WTs is investigated in [20,21]. The WT model is linearized, and the sampling time is 0.1 s, which is not easy to implement in the WPP controller for engineering applications. Generally, the required predictive information mainly refers to the wind speed. Wind speed forecasting has been studied in [22–25]. The 1 min wind speed forecasting data is used in the power dispatch strategy [18], and the minute level wind speed forecasting error can be achieved to less than 10 % [26].

As introduced in the literature review, impressive achievements have been made in the active power dispatch for WPP, while knowledge gaps still exist in the following aspects.

- (1) Dynamic wake effect with time delay has not been considered in the previous active power dispatch model, resulting in the inaccuracy of the optimization results.
- (2) The advantage of RSC in storing kinetic energy is overemphasized so that its disadvantage of further aggravating wake effect has been ignored.

In this paper, an active power dispatch strategy for WPP based on the nonlinear MPC (NMPC) is proposed to provide an operating condition reference for each WT and prepare the WPP to participate in system frequency regulation. The main contributions of this paper can be

summarized as follows.

- (1) The temporary and sustained APSCs of WPP are analyzed. The impacts of excessively increasing the priority of the RSC on that capabilities are revealed, and the evaluation indicators of temporary and sustained APSCs are presented.
- (2) An active power dispatch strategy for WPP based on NMPC considering dynamic wake effect is proposed, solving the time delay and nonlinearity in the optimization problem and simultaneously improving the temporary and sustained APSCs without sacrificing blade deflection.
- (3) A bi-level control framework is proposed. The operating point optimization is conducted in the WPP level, and the active power control in the WT level guides how the WT should act during the sampling interval of the WPP controller.
- (4) Extensive case studies are performed in scenarios of different wind conditions and power references, validating the theoretical analysis and the superiority of the proposed scheme.

The rest of the paper is organized as follows. In Section 2, the models of WT and wake effect are established, and the APSC of WPP in different timescales is analyzed. Section 3 presents the bi-level control framework. In Section 4, the NMPC-based active power dispatch and coordinated active power control of WT are designed in detail. Case studies are performed and discussed in Section 5. Conclusions are drawn in Section 6.

2. Problem description

2.1. Wind turbine model

The mechanical power captured by the wind turbine from the wind energy, P_{wm} , is shown [27]

$$P_{wm} = \frac{1}{2} \rho \pi R_w^2 C_p(\lambda, \beta) v_w^3 \quad (1)$$

where ρ , R_w , v_w , C_p , β , and λ are the air density, rotor radius, wind speed, power coefficient, pitch angle, and tip-speed ratio, respectively. The tip-speed ratio is defined as

$$\lambda = \frac{\omega_w R_w}{v_w} \quad (2)$$

where ω_w denotes the rotor speed of the WT.

The characteristics of $C_p(\lambda, \beta)$ of a National Renewable Energy Laboratory (NREL) 5 MW WT are shown in Fig. 1. It can be obtained that the optimal tip speed ratio of the WT, λ_{opt} , equals 7.5.

2.2. Dynamic wake effect model

Wind energy extraction of wind turbine always accompanies with a

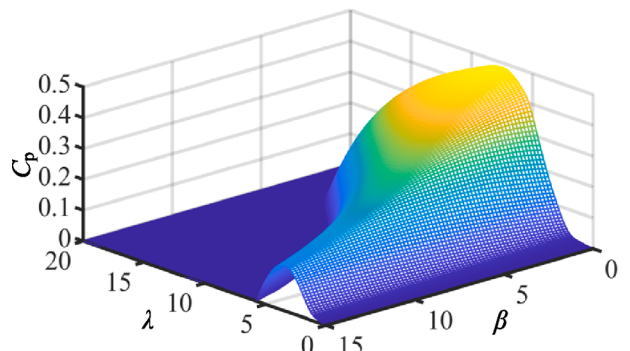


Fig. 1. Power coefficient characteristics of WT.

wake behind the turbine. It has been shown in [28] that a good approximation of the meandering is to consider the wake center as a passive tracer which moves downwind with the mean wind speed. The wake center, expansion and deficit at a given point p downstream from a turbine at time t_1 is defined by the wind field at the turbine and its coefficient of thrust at the time of tracer release, t_0 ,

$$t_0 = t_1 - d/v_w \quad (3)$$

where d is the longitudinal distance between the upwind turbine and point p .

Assuming that a WPP is divided into n_{row} rows n_{col} columns according to the wind direction. Let $\tau = t_1 - t_0$. The wake effect of a turbine is presented in Fig. 2, and the deficit from the j th column i th row of WT (hereinafter called the 'WT _{i,j} ') can be approximated as [29]

$$v_{wi,j}(t) = v_{w1,j}(t - \tau_{1,j}) \prod_{m=1}^{i-1} \left[1 - \frac{1}{2} C_{T,m,j}(t - \tau_{mi,j}) \left(1 + \frac{d_{mi,j}}{4R_w} \right)^{-1} \right] \quad (4)$$

where $v_{wi,j}$ denotes the wind velocity of WT _{i,j} , $v_{w1,j}$ denotes the upstream wind velocity, $\tau_{mi,j}$ denotes the delay time of the wake from WT _{m,j} to WT _{i,j} , $C_{T,m,j}$ denotes the thrust coefficient of the WT _{m,j} , $d_{mi,j}$ denotes the longitudinal distance between WT _{m,j} and WT _{i,j} .

The thrust coefficient $C_T(\lambda, \beta)$ of an NREL 5 MW WT is shown in Fig. 3, and these nonlinear characteristics are the foundation of the following problem analysis.

2.3. Problem analysis

The strength of wake effect is determined by the thrust coefficient of the WT, and C_T is nonlinear with λ and β , shown in Fig. 3. The two main deloading strategies of WTs, which are rotor speed control (RSC) and pitch angle control (PAC), change the mechanical power of WT by adjusting λ and β respectively. Therefore, different deloading strategies have different influences on the wake effect, and then affect the characteristics of the output power of the WPP. In this section, this issue is analyzed in detail.

It can be obtained in (4) that the velocity profile of the wake generated by WT decreases with the increase of C_T , assuming other parameters remain unchanged. As is illustrated in Fig. 3, C_T decreases with the increase of β ($\lambda = 7.5$) and decreases with the decrease of λ ($\beta = 0$). Thus, compared with PAC, the RSC has an opposite impact on wake effect. The RSC will further enhance the wake effect, reducing the wind velocity of the downstream WT. However, the PAC will weaken the wake effect, releasing the wind energy to the downstream WT during deloading. In other words, if the upstream WT has a curtailed power ΔP from MPPT condition, the wind velocity of the downstream WT will change. Generally, the sum of power changes of multiple WTs is not equal to ΔP even if the MPPT operation is still adopted by the downstream WTs. From a single WT's point of view, more kinetic energy can be stored with RSC than that with PAC, which can be used during the electromechanical timescale. However, from the perspectives of WPP, the high priority of RSC would reduce the increasable active power of WPP since it will enhance the wake effect.

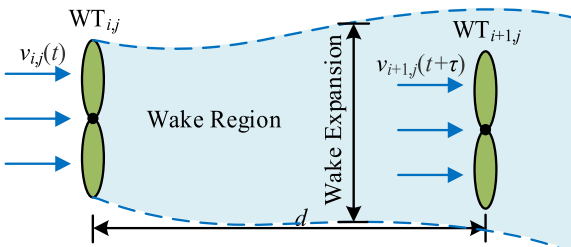


Fig. 2. Wake effect of a turbine.

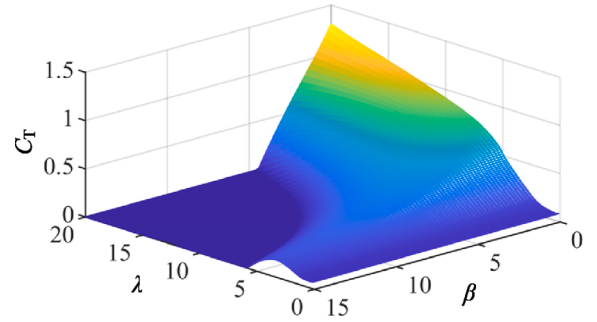


Fig. 3. Thrust coefficient characteristics of WT.

If the MPPT strategy is adopted, the power output of WTs can be expressed as

$$P_{wi,j}^{\text{MPPT}} = K_{\text{opt}} v_{i,j,\text{MPPT}}^3 \quad (5)$$

where $P_{wi,j}^{\text{MPPT}}$ denotes the maximum power of the WT _{i,j} , K_{opt} denotes the MPPT control coefficient, $v_{i,j,\text{MPPT}}$ denotes the wind velocity of the WT _{i,j} with MPPT control. Afterwards, the output power of WPP with MPPT control, $P_{\text{WPP}}^{\text{MPPT}}$, can be obtained

$$P_{\text{WPP}}^{\text{MPPT}} = \sum_{j=1}^{n_{\text{col}}} \sum_{i=1}^{n_{\text{row}}} P_{wi,j}^{\text{MPPT}} \quad (6)$$

If the deloading control is adopted by all the WTs, tip speed ratio and pitch angle of WTs are regulated to adjust the captured wind energy to keep the power balance. Thus, the curtailed power of each WT can be deduced as

$$\begin{cases} P_{wi,j} = P_{wi,j,\text{max}} - P_{wi,j} \\ P_{wi,j,\text{max}} = K_{\text{opt}} v_{wi,j}^3 \end{cases} \quad (7)$$

where $P_{wi,j}$ denotes the increasable power of the WT _{i,j} , $P_{wi,j}$ denotes the output power of the WT _{i,j} with deloading control, $P_{wi,j,\text{max}}$ denotes the maximum power of the WT _{i,j} . Then, the output power of WPP, P_{WPP} , can be obtained

$$P_{\text{WPP}} = \sum_{j=1}^{n_{\text{col}}} \sum_{i=1}^{n_{\text{row}}} P_{wi,j} \quad (8)$$

Due to the change of the tip speed ratio and pitch angle of WTs, the wake distribution in the WPP is changed. Thus, the $v_{wi,j}$ does not equal $v_{i,j,\text{MPPT}}$ except for the WTs in the first row, by which means the WT's increasable power is not the expected value. The expected increasable power of the WT _{i,j} , $P_{wi,j}^{\text{exp}}$, is shown as

$$P_{wi,j}^{\text{exp}} = P_{wi,j}^{\text{MPPT}} - P_{wi,j} \quad (9)$$

According to (4), though the upstream wind velocity is the same, the wind velocity of the WT _{i,j} is still coupled with the thrust coefficient of the upstream WT, which varies with the change of the deloading control strategy. This coupling features among WTs caused by wake effect increases the complicacy of the output characteristics of multiple WTs as well as the difficulty in power control of WPP.

The curtailed power in (7) can be considered as the increasable power. From the WPP's point of view, the increasable power, P_{WPPin} , and expected increasable power, $P_{\text{WPPin}}^{\text{exp}}$, can be obtained according to (6)-(9)

$$P_{\text{WPPin}} = \sum_{j=1}^{n_{\text{col}}} \sum_{i=1}^{n_{\text{row}}} P_{wi,j} \quad (10)$$

$$P_{\text{WPPin}}^{\text{exp}} = P_{\text{WPP}}^{\text{MPPT}} - P_{\text{WPP}} \quad (11)$$

The $P_{\text{WPPin}}^{\text{exp}}$ is introduced as the evaluation indicator of the sustained APSC of WPP. The inconsistency of the increasable power and expected

increasable power of WPP increases the difficulty of the deloading control of WPP. Since the adopt of RSC will reduce the wind velocity of the downstream WT, assuming the downstream WT is $WT_{i,j}$, the $P_{wi,j,\max}$ and $P_{wi,j}$ in (7) will be decreased. As a result, the increasable power of the whole WPP, P_{WPPin} , will be reduced.

Due to the time delay effect of wind, the timescale of the change of wake distribution is usually on the order of minutes. Although WPP with each deloading control strategy can return back to the MPPT operation eventually, which needs a few minutes, the P_{WPPin} within minute timescale is reduced. Generally, the stored kinetic energy can be released in few seconds, which usually serves as the inertial response to power system. This phenomenon jeopardizes the frequency stability of power system. When the frequency drops, the WPP may not be able to provide power system with primary frequency regulation.

It is worth noting that the stored kinetic energy in wind turbine is not considered in the increasable power because it is usually used for the active power support during the electromechanical transient timescale. The total stored kinetic energy of the WPP, E_{WPP} , which is selected as the evaluation indicator of the WPP's temporary APSC, can be expressed as

$$\left\{ \begin{array}{l} E_{WPP} = \sum_{j=1}^{n_{col}} \sum_{i=1}^{n_{row}} 0.5 J_{wi,j} (\omega_{wi,j}^2 - \omega_{opti,j}^2) \\ \omega_{opti,j} = \frac{\lambda_{opt} v_{wi,j}}{R_w} \end{array} \right. \quad (12)$$

where $J_{wi,j}$ denotes the rotational inertia of $WT_{i,j}$, λ_{opt} denotes the optimal tip speed ratio of WT, $\omega_{opti,j}$ denotes the optimal rotor speed of $WT_{i,j}$ with MPPT strategy.

Furthermore, if the wind speed of downstream WT is increased due to the upstream WT adopting PAC, it is possible for WPP to improve the temporary and sustained APSCs simultaneously.

3. Bi-level control framework

In order to improve the capabilities of temporary and sustained power support comprehensively, an active power dispatch strategy for WPP based on NMPC is proposed. The control framework is shown in Fig. 4, which is divided into two parts. The WPP controller is responsible for the operation optimization and control instructions generation. The WT controller should track the power and pitch angle command value and adjust WT's rotor speed and pitch angle in real-time.

Specifically, in WPP layer, the predictive model including the wind speed and the operating statuses of WTs considering dynamic wake effect is established. The operating conditions of WTs are optimized with the objective of maximizing the stored kinetic energy and minimizing the pitch angle variation. Meanwhile, the increasable active power in minute timescale is guaranteed by the constraints. If the time delay of

wake effect is ignored, it is obtained that the wake distribution can be improved immediately with the change of WTs' statuses, and the WPP can reach the optimal operating status rapidly. However, it takes time for WTs to change the spatial distribution of the wake, which will cause non-negligible errors to the traditional optimization methods. As a result, the particle swarm optimization (PSO) and NMPC methods are utilized to solve the time delay and nonlinearity simultaneously. The time taken for the wind to flow from the upstream WT to the downstream WT is contained in the control horizon of receding horizon optimization. The optimization at each instant k will take the overall performance during the control horizon into account. The sampling time is determined by the delay time of the wake, and the calculation duration of the optimization algorithm should be shorter than the sampling time to ensure its effectiveness. As a result, the wind speed fluctuations during the sampling interval is neglected in the NMPC algorithm. If the real-time wind speed is different from the predicted one, the WTs will inevitably deviate from the optimal operating point. Thus, the coordinated active power control is required.

The randomness and intermittence of wind sources lead to the change of operating conditions of WTs. Therefore, the active power control is accomplished in the WT layer to adjust to the wind source fluctuations in real-time. The optimization results in the WPP layer are used as a steady state benchmark for the coordinated active power control. Through setting different priorities of the RSC and PAC based on the operating conditions of WTs, the impact of the wind speed fluctuations on the APSC of WTs can be reduced during the sampling interval of WPP controller. If the wind speed increases, the priority of the RSC is higher than that of the PAC. On the contrary, the PAC should be activated as far as possible if the wind speed decreases. If the rotor speed is lower than the optimal value, the P_{ref} will decrease and this information will be reported to WPP controller. As a result, other WTs will increase the P_{ref} to guarantee the output power of the whole WPP.

Since the NMPC based WPP controller only provides the reference of the operating status of WTs, researches on the inertial response and frequency regulation strategy for WPP and WTs are still applicable to the proposed active power dispatch framework.

4. Active power dispatch strategy for WPP

The main purpose of the active power dispatch strategy is to optimize the operation states of WTs to keep a balance between the abilities of temporary power support and sustained power support. Taking the time delay of wake effect into account, it can be transformed into a receding horizon optimization problem in a finite time domain. An active power dispatch strategy based on nonlinear MPC is proposed, and the detailed design steps are as follows.

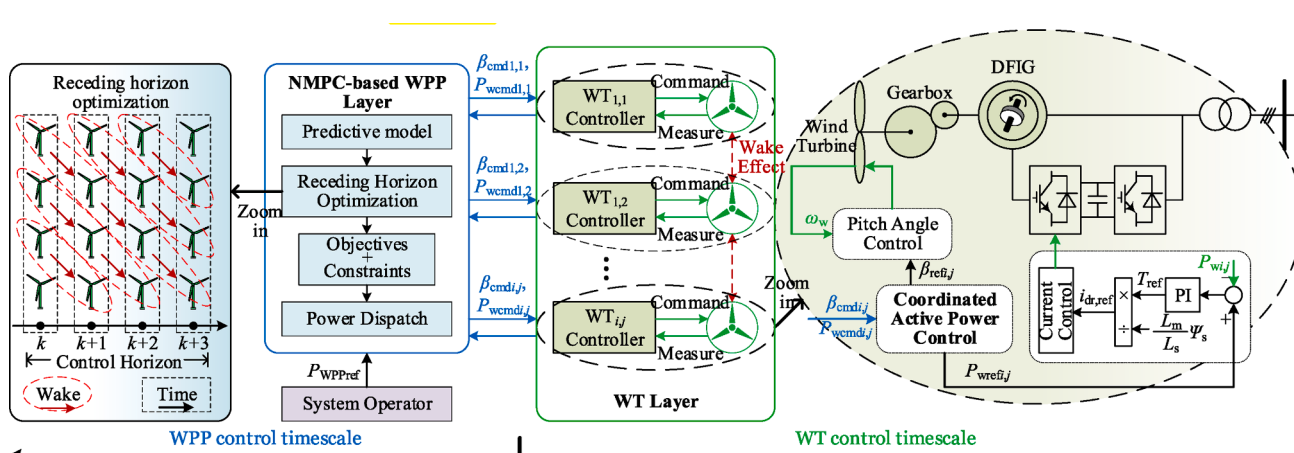


Fig. 4. Bi-level control framework of the proposed active power dispatch strategy.

4.1. Predictive model

In the NMPC framework, a predictive model has to be established to predict the future behavior of the variables to be controlled.

According to (1)-(4), discrete active power output model of $WT_{i,j}$ can be obtained

$$\left\{ \begin{array}{l} P_{wi,j}(k) = \frac{1}{2} \rho \pi R_{wi,j}^2 \mu C_{P,i,j} v_{wi,j}^3(k) \\ C_{P,i,j}(k) = h_1[\lambda_{ij}(k), \beta_{ij}(k)] \\ v_{wi,j}(k) = v_{w1,j}(k+1-i) \prod_{m=1}^{i-1} \left[1 - \frac{1}{2} C_{T,m,j}(k+m-i) \left(1 + \frac{d_{mi,j}}{4R_w} \right)^{-1} \right] \\ C_{T,i,j}(k) = h_2[\lambda_{ij}(k), \beta_{ij}(k)] \\ \lambda_{ij}(k) = \frac{\omega_{wi,j}(k) R_w}{v_{wi,j}(k)} \end{array} \right. \quad (13)$$

where μ is the energy conversion efficiency of the WT from mechanical power to electrical power, h_1 is the nonlinear function of $\lambda_{ij}(k)$ and $\beta_{ij}(k)$ to $C_{P,i,j}(k)$ shown in Fig. 1, h_2 is the nonlinear function of $\lambda_{ij}(k)$ and $\beta_{ij}(k)$ to $C_{T,i,j}(k)$ shown in Fig. 3, $i, m \in N_{\text{row}}, j \in N_{\text{col}}$, N_{row} is $\{1, 2, \dots, n_{\text{row}}\}$, N_{col} is $\{1, 2, \dots, n_{\text{col}}\}$. The time delay effect of the wind is taken into account in the third sub-formula of (13). The $v_{wi,j}(k)$ is calculated according to the upstream wind speed and the thrust coefficient of all the upstream WTs at the time step when the wind flow through that WT. It is noted that the values of the time delay τ_{adj} between two adjacent WTs are assumed to be equal in the discrete model. The sampling time of the controller is set according to the average value of the time delay, so that the moment of $t + \tau_{\text{adj}}$ in the continuous model can be discretized as the time step $k + 1$ in the discrete model. Although the accuracy of the description of the dynamic wake effect is compromised by the simplification of the delay, the computational burden on the algorithm can be decreased.

According to (12) and (13), by integrating all WTs, the discrete nonlinear state space model of WPP can be obtained

$$\left\{ \begin{array}{l} \mathbf{x}(k+1) = f[\mathbf{x}(k), \mathbf{u}(k), d(k+1)] \\ y(k) = g[\mathbf{u}(k)] \end{array} \right. \quad (14)$$

where $\mathbf{x}(k) = [v_{w1,1}(k), v_{w1,2}(k), \dots, v_{wn_{\text{row}},n_{\text{col}}}(k)]$ is the state variable of the system, $\mathbf{u}(k) = [P_{w1,1}(k), P_{w1,2}(k), \dots, P_{wn_{\text{row}},n_{\text{col}}}(k), \beta_{1,1}(k), \beta_{1,2}(k), \dots, \beta_{n_{\text{row}},n_{\text{col}}}(k)]$ is the control variable of the system, $d(k+1) = v_{w\text{pre}}(k+1)$ is the disturbance of the system, $y(k) = E_{\text{WPP}}(k)$ is the output of the model, f is the nonlinear function of $\mathbf{x}(k)$, $\mathbf{u}(k)$ and $d(k+1)$ to $\mathbf{x}(k+1)$, g is the nonlinear function of $\mathbf{u}(k)$ to $y(k)$.

For modern wind turbines, there is, in general, an anemometer mounted on the top of the nacelle, so that the real-time turbine top wind speed $v_{w1,1}$ to $v_{wn_{\text{row}},n_{\text{col}}}$ can be sensed [30,31] which are regarded as the state variables. As reviewed in the Introduction, the relative error of the 1-min wind speed forecasting can be achieved within 10 % [26]. A forecasting model with 10 % error is applied. Thus, the predicted value of the upstream wind speed of the WPP, $v_{w\text{pre}}$, can be obtained.

Based on the instant k , the system state variables at instant $k + 1$ to $k + N_p$ can be predicted by the predictive model shown in

$$\left\{ \begin{array}{l} \mathbf{X}(k+N_p) = F[\mathbf{x}(k), \mathbf{U}(k), \mathbf{D}(k+1)] \\ \mathbf{Y}(k+N_p) = G[\mathbf{U}(k)] \end{array} \right. \quad (15)$$

where N_p is the number of prediction horizon point, $\mathbf{X}(k+N_p) = [\mathbf{x}(k+1) \ \mathbf{x}(k+2) \ \dots \ \mathbf{x}(k+N_p)]^T$, $\mathbf{Y}(k+N_p) = [\mathbf{y}(k+1) \ \mathbf{y}(k+2) \ \dots \ \mathbf{y}(k+N_p)]^T$, $\mathbf{U}(k) = [\mathbf{u}(k) \ \mathbf{u}(k+1) \ \dots \ \mathbf{u}(k+N_p-1)]^T$, $\mathbf{D}(k+1) = [d(k+1) \ d(k+2) \ \dots \ d(k+N_p)]^T$, F is the nonlinear function of $\mathbf{x}(k)$, $\mathbf{U}(k)$ and $\mathbf{D}(k+1)$ to $\mathbf{X}(k+N_p)$, G is the nonlinear function of $\mathbf{U}(k)$ to $\mathbf{Y}(k+N_p)$.

4.2. Receding horizon optimization of WPP

Generally, the steady state output of WPP should track the command from system operator. The output power could be adjusted with the variation of system frequency to provide frequency support for power system. Therefore, it is significant that the required active power can be increased or decreased to participate in the frequency regulation.

Though kinetic energy stored in turbines can be charged as the buffer energy for frequency regulation, the over-speed of upstream WTs will damage the potential output capability of WPP considering wake effects. Thus, it is necessary to coordinate RSC and PAC from the perspective of the whole WPP.

Moreover, the problem of the increase in mechanical wear and reduction of WT's life caused by frequently change of pitch angle, which is contained in the control variables $\mathbf{U}(k)$, should be considered reasonably.

Based on the analysis above, the optimization problem of the load sharing of WTs can be formulated as

$$\min J = [\mathbf{U}(k+1) - \mathbf{U}(k)] \mathbf{R}_U - \mathbf{Y}(k+N_p) \mathbf{Q}_Y \quad (16)$$

where \mathbf{Q}_Y and \mathbf{R}_U are the symmetric weighting matrix.

The constraints are presented as follows.

(1) The rotor speed constraints: The stored kinetic energy can be released in frequency regulation, but the WT can only decelerate to the left-side of the maximum power point temporarily, which is always accompanied by a recovery process [32]. Consequently, the rotor speed of each WT should be guaranteed between the optimal value and the maximum value in power dispatch.

$$\omega_{\text{opti},j} \leq \omega_{wi,j} \leq \omega_{\text{max}} \quad (17)$$

where $\omega_{\text{opti},j}$ is the optimal rotor speed of $WT_{i,j}$, ω_{max} is the maximum value of rotor speed.

(2) The power constraints: The active power output of each WT should be guaranteed between the minimum value and the nominal value. The minimum value of the active power of WTs is set to 0.1p.u..

$$P_{w\text{min}} \leq P_{wi,j} \leq P_{w\text{nom}} \quad (18)$$

where $P_{w\text{min}}$ is the minimum value of the active power of WT, $P_{w\text{nom}}$ is the nominal value of WT.

(3) The power reference tracking constraints: The active power of WPP should track the reference value provided by the system operator.

$$P_{\text{WPP}} = P_{\text{WPRef}} \quad (19)$$

(4) The increasable power constraints: The WPP should have the ability to increase the active power to $P_{\text{WPP}}^{\text{MPPT}}$ deduced in (6). The output power of WPP with MPPT control is acquired through the historical data.

$$\sum_{j=1}^{n_{\text{col}}} \sum_{i=1}^{n_{\text{row}}} P_{wi,j,\text{max}} \geq P_{\text{WPP}}^{\text{MPPT}} \quad (20)$$

In this paper, the PSO algorithm, which is widely used in the nonlinear optimization problem, is applied to NMPC as the optimization algorithm, and constraints are transformed into the penalty function, shown as

$$\left\{ \begin{array}{l} C_{\text{pen}} = \gamma_1 C_{\text{pen1}} + \gamma_2 C_{\text{pen2}} + \gamma_3 C_{\text{pen3}} + \gamma_4 C_{\text{pen4}} \\ \gamma_1 + \gamma_2 + \gamma_3 + \gamma_4 = 1 \end{array} \right. \quad (21)$$

$$C_{\text{pen1}} = \max \left[\sum_{j=1}^{n_{\text{col}}} \sum_{i=1}^{n_{\text{row}}} (\omega_{\text{opti},j} - \omega_{wi,j}) (\omega_{\text{max}} - \omega_{wi,j}), 0 \right] \quad (22)$$

$$C_{\text{pen2}} = \max \left[\sum_{j=1}^{n_{\text{col}}} \sum_{i=1}^{n_{\text{row}}} (P_{w\text{min}} - P_{wi,j}) (P_{w\text{nom}} - P_{wi,j}), 0 \right] \quad (23)$$

$$C_{\text{pen}3} = |P_{\text{WPPref}} - P_{\text{WPP}}| \quad (24)$$

$$C_{\text{pen}4} = \max \left(P_{\text{WPP}}^{\text{MPPT}} - \sum_{j=1}^{n_{\text{col}}} \sum_{i=1}^{n_{\text{row}}} P_{\text{wi},j,\text{max}}, 0 \right) \quad (25)$$

where C_{pen} denotes the penalty function, $C_{\text{pen}1}$, $C_{\text{pen}2}$, $C_{\text{pen}3}$, $C_{\text{pen}4}$ denote the four parts of penalty function corresponding to (22)-(25), γ_1 , γ_2 , γ_3 , γ_4 denote the weight coefficients of the constraints, whose values are positive.

Then, the objective function can be rewritten as

$$\min J = [\mathbf{U}(k+1) - \mathbf{U}(k)] \mathbf{R}_{\text{U}} - \mathbf{Y}(k+N_p) \mathbf{Q}_{\text{Y}} + C_{\text{pen}} \quad (26)$$

The optimization problem can be solved by applying PSO algorithm in NMPC scheme, and the design of WPP controller is finished.

4.3. Coordinated active power control of WT

The receding horizon optimization implements the pitch angle and active power dispatch for the next sampling interval. It optimizes the schedule of all WTs in the WPP. However, the operating condition of WPP is time-varying with the fluctuations of wind speed. Since the time delay of the wake is approximately minutes level, the active power control of the WT is intended to guide how the WT should act when it necessarily deviates from the optimal operating point due to intra-minute wind speed fluctuations. In other words, the purpose of the coordinated active power control of WT is to tackle the load-sharing problem within the sampling interval of NMPC.

The variation of wind speed can be divided into two categories: wind speed increases or decreases. Due to the time delay of wind flow, the wind speeds of WTs in different rows will not increase and decrease at the same time. Since the steady-state operating point is optimized by the WPP controller, the WT control observe the following principles:

(1) If the wind speed increases, the active power and pitch angle references of the WT can remain unchanged, and the rotor speed should be accelerated first to keep following the power reference and avoid the irreversible blade pitch fatigue meanwhile. If the rotor speed reaches the upper limit, pitch angle control should be activated to further reduce the captured wind energy. In this situation, the active power reference remains unchanged and pitch angle reference is modified by the PAC.

(2) If the wind speed decreases, the active power reference and rotor speed of the WT can remain unchanged, and the pitch angle should be reduced first to enhance the capture of wind energy. If the pitch angle is equal to 0, the rotor speed of the WT should be decelerated. Provided that the wind speed drops sharply, the affected WTs cannot track the active power reference even if they return to the maximum power point. Afterwards, the active power reference should be equal to the maximum power, shown as

$$P_{\text{wref},i,j} = \min \left(P_{\text{wi},j}^{\text{MPPT}}, P_{\text{wref},i,j} \right) \quad (27)$$

In this situation, the WPP controller should adjust the active power references of other WTs according to the cube of wind speed, shown in

$$P_{\text{wref},i,j} = P_{\text{wcmd},i,j} - \Delta P_{\text{WPP}} \frac{V_{\text{wi},j}^3}{\sum_{j=1}^{n_{\text{col}}} \sum_{i=1}^{n_{\text{row}}} V_{\text{wi},j}^3} \quad (28)$$

where ΔP_{WPP} denotes the active power deviation of WPP.

In summary, the RSC has a higher priority than PAC when wind speed increases, and the PAC has a higher priority than RSC when wind speed decreases. If all WTs generating their maximum power still cannot meet the power command, MPPT control shall remain in use, and the WPP operator should report this to the system operator.

4.4. Flowchart of the proposed strategy

The flowchart of the proposed active power dispatch strategy is

shown in Fig. 5.

The flowchart includes NMPC in WPP controller and coordinated control in WT controller. When the sampling time of NMPC comes, the wind speed, rotor speed and pitch angle of each WT will be sampled and written into WPP controller. Along with the predicted upstream wind speed, the data used by receding horizon optimization are updated. Afterwards, the PSO algorithm is performed, including initialization and looping iteration for optimization. If the iteration is finished, output the first control variable vector $u(k)$, which consists of the active power and pitch angle reference of WTs.

During the sampling interval of NMPC in WPP controller, the coordinated active power control of WT is presented to adapt to the wind speed variation. It is notable that the wind speed variation is converted into the mechanical power variation in the flowchart in Fig. 5, which is easier to conducted for the controller.

5. Case study

To verify the validity of the theoretical analysis effect of the proposed control strategy on WPP's operation, different strategies are implemented in a 100 MW WPP composed of twenty NREL 5 MW WTs. The WPP and wind field are realized based on RT-LAB OP5700 platform, shown in Fig. 6. The configuration of the WPP is shown in Fig. 7. The distance between the two adjacent WTs is 600 m. The 20 WTs are divided into 4 rows and 5 columns according to the wind direction. They are clustered into 4 groups in the case studies according to the number of rows where the WT is located, and the single machine equivalent model is used in each group, which are called WT1 to WT4 respectively.

5.1. Different deloading control strategies analysis

The effects of RSC and PAC on the output power of WPP and the inconsistency of the ROPC of WPP and WTs can be explicated by a brief case study. Suppose a WPP has four WTs in the same wind direction, WT1 to WT4 from upstream to downstream. The upstream wind speed is 9.5 m/s. The RSC and PAC are adopted by the four WTs respectively, and the ROPC of 4 WTs are the same.

The mechanical power of WPP and each WT with different ROPC of WTs are shown in Fig. 8. The MPPT control is adopted by WTs and the mechanical power of each WT is equal in the first two bars. As the ROPC of WT increases, the mechanical power of WT1 with RSC and PAC stay the same. However, mechanical power of WT2 and WT3 with RSC are reduced distinctly compared to that with PAC, because WT1 releases considerable wind energy to the downstream WTs by increasing its pitch angle, facilitating the overall power output capability of the WPP. To further exhibit the characteristics, the ROPC of WPP versus ROPC of WTs curves are shown in Fig. 9, with RSC and PAC.

As can be seen in Fig. 9, there is a significant difference in the influence of the two deloading strategies on the output characteristics of WPP. The ROPC of WPP with RSC is higher than that with PAC. The difference between the ROPC of WPP with RSC and PAC achieves about 11 % when the ROPC of WTs is 6 %. When the ROPC of WT reaches 10 %, the ROPC of WPP is 15.51 % with RSC and 2.26 % with PAC. Therefore, the sustained APSC of WPP will be reduced by RSC while it will be enhanced by PAC. It should be noted that using only RSC or only PAC is also the control boundary of the WTs' operating statuses.

5.2. Different active power dispatch strategies analysis

To analyze the effect of different wind conditions on the performance of proposed strategy, the constant wind and turbulent wind scenarios are set. Furthermore, the variable power reference scenario is set up to demonstrate that WPP can track the power reference accurately. The wake model from the SimWindFarm toolbox is used in the cases.

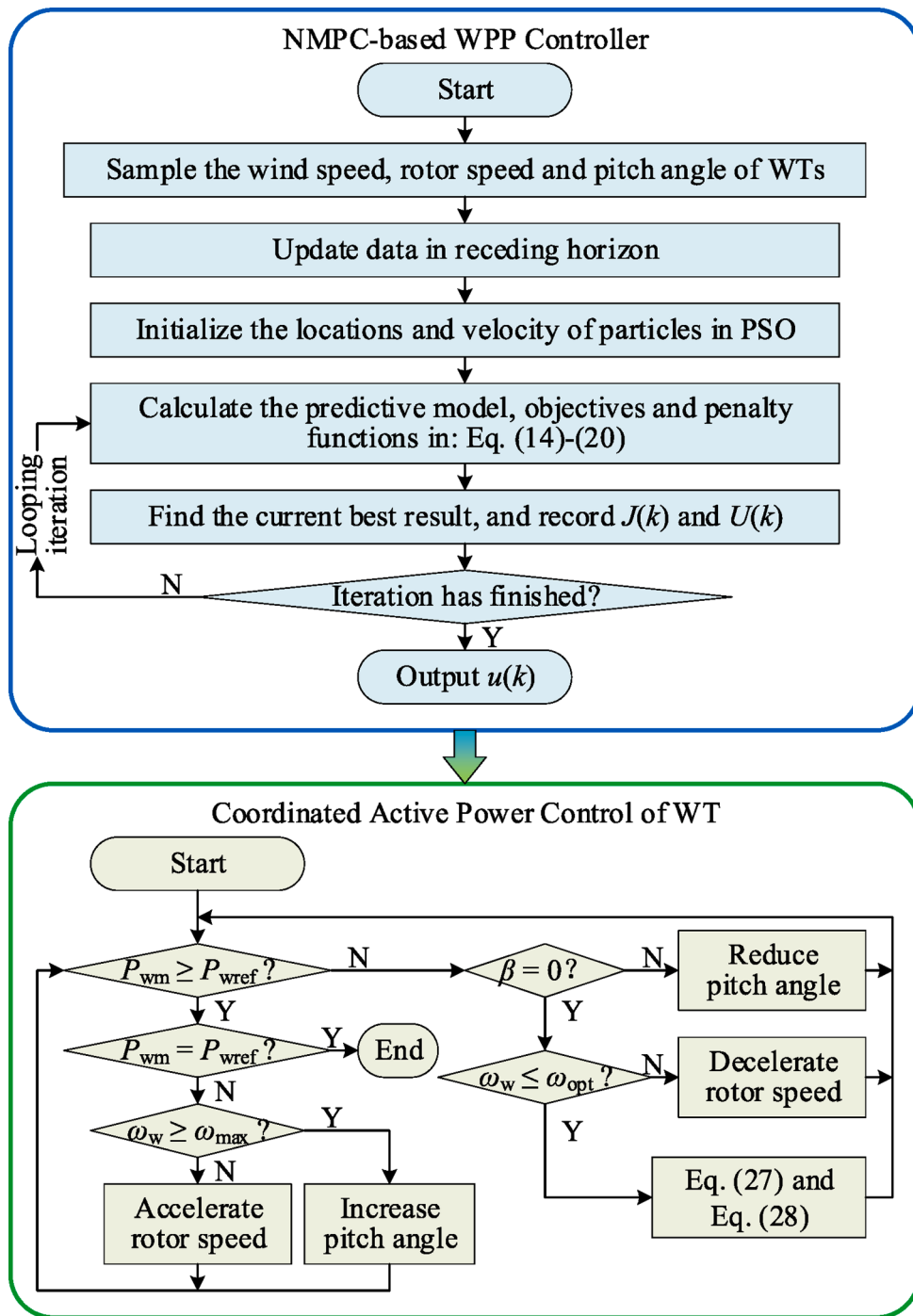


Fig. 5. Flowchart of the proposed active power dispatch strategy.

5.2.1. Constant wind with constant power reference

To test the performance of NMPC, the scenario of constant wind with dynamic wake effect is imitated. The upstream wind speed is set to 10 m/s. The active power reference of WPP is 0.45p.u.. The active power regulation strategy proposed in [17], called RSC prior strategy, is compared in the following cases.

As shown in Fig. 10 (a), the mean wind speeds of the WT2 to WT4 with NMPC strategy are about 9 m/s, 8.6 m/s and 8.3 m/s respectively, which are larger than that with MPPT and RSC prior strategies, shown in Fig. 10 (b) and (c). As a result of the WT operating status optimization considering dynamic wake effect, the wind speeds of downstream WTs are improved.

From Fig. 11 (a), the active power of WPP with MPPT strategy is

0.478p.u., and the active power output of WPP with NMPC and RSC prior strategies can track the reference value, which is 0.45p.u.. The amount of stored kinetic energy of WPP with the two strategies have little difference, shown in Fig. 11 (b), and the rotor speeds of WT1 and WT3 with NMPC are larger than that with RSC prior strategy, shown in Fig. 11 (d1) to (d2). In Fig. 11 (c), the increasable power of WPP with NMPC is larger than that with RSC prior strategy obviously, whose mean values are about 0.06p.u. and 0.01p.u. respectively. Thus, the sustained APSC of the WPP with NMPC is improved effectively. It is notable that this advantage is based on the activation of pitch angle control, shown in Fig. 11 (e1). In Table 1, the total deflection of pitch angle with NMPC and RSC prior strategies are approximately equal, and the blade deflections of WTs with NMPC are more average than that with RSC prior

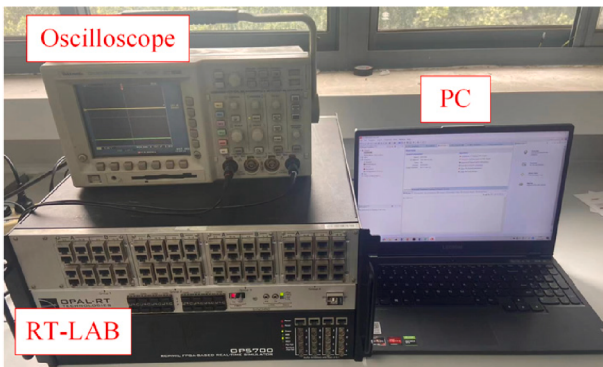


Fig. 6. RT-LAB platform.

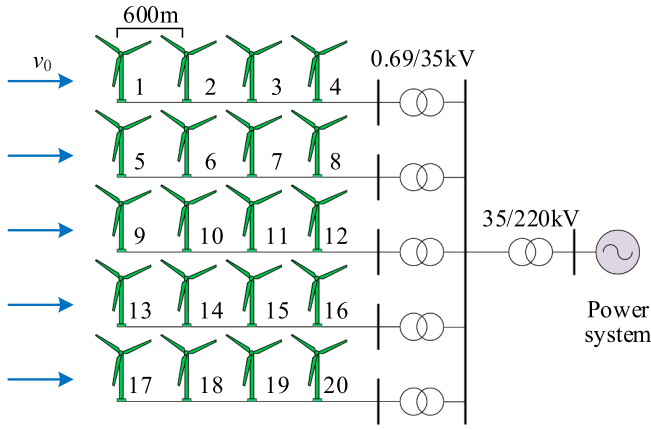


Fig. 7. Configuration of the test WPP.

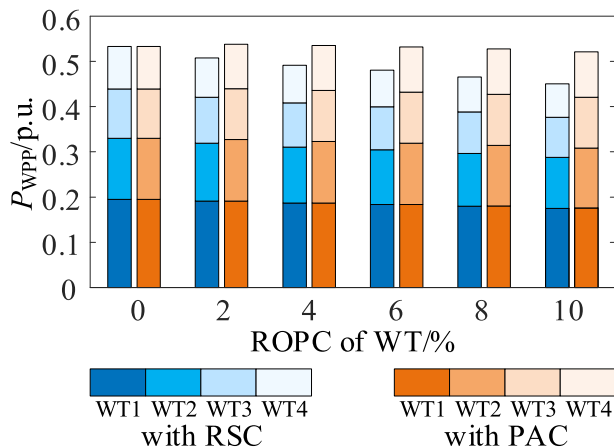


Fig. 8. Mechanical power of WPP with different ROPC of WTs.

strategy.

5.2.2. Turbulent wind with constant power reference

To further verify the effect of the proposed control strategy on WPP's operation in turbulent wind, a more realistic scenario, different strategies are implemented in this case. The simulation time of this case is 800 s, the mean wind speed is 9 m/s, and the turbulence intensity is 0.02, as shown in Fig. 12. The active power reference is 0.32 p.u..

The operation comparison is shown in Fig. 13. As can be seen in Fig. 13 (a), the active power outputs of the WPP with NMPC and RSC prior strategies track the reference value. The stored kinetic energy of the WPP with different control strategies are shown in Fig. 13 (b). It can

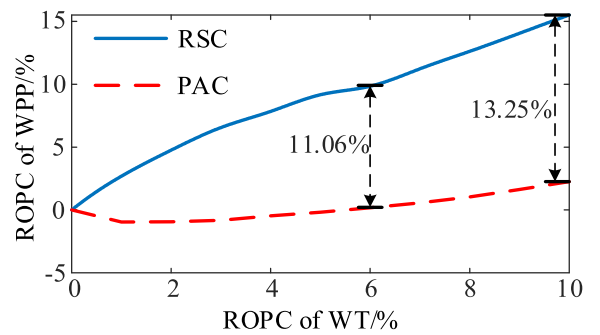


Fig. 9. The ROPC of WPP versus ROPC of WTs curves.

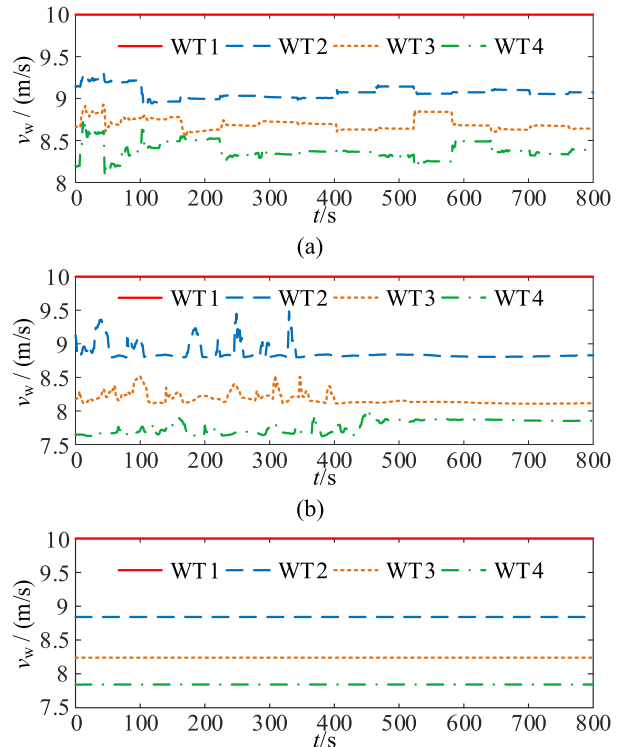


Fig. 10. Wind speed of each WT with (a) NMPC strategy, (b) RSC prior strategy, (c) MPPT strategies.

be obtained that the stored kinetic energy with the proposed NMPC strategy is larger than that with the RSC prior strategy during most of the time. The stored kinetic energy of WPP with MPPT strategy is maintained at about 0. As illustrated in Fig. 13 (c), the increasable power of WPP with the proposed strategy is larger than that with RSC prior strategy before $t = 400$ s, and the increasable power of WPP is similar with the two strategies after $t = 400$ s due to the variation of wind speed. It is noted that the results shown in Fig. 13 (c) are the instantaneous value. Since the kinetic energy can be charged as the buffer energy, the WPP has the ability to increase active power output even if P_{WPPin} equals 0. Therefore, the mean value of P_{WPPin} responds more realistically to the sustained increasable power of WPP. The mean values of P_{WPPin} every 60 s are shown in Fig. 13 (c), and the P_{WPPin} is improved by 104.88 % in average with the proposed strategy. It can be obtained that the WPP with the proposed strategy has a stronger temporary and sustained capabilities to support the frequency. The rotor speeds of each WT in the WPP are shown in Fig. 13 (d1) to (d3), which are with NMPC, RSC prior and MPPT strategy respectively. It can be seen that the WTs' rotor speeds with the proposed strategy are larger than that with other strategies in general.

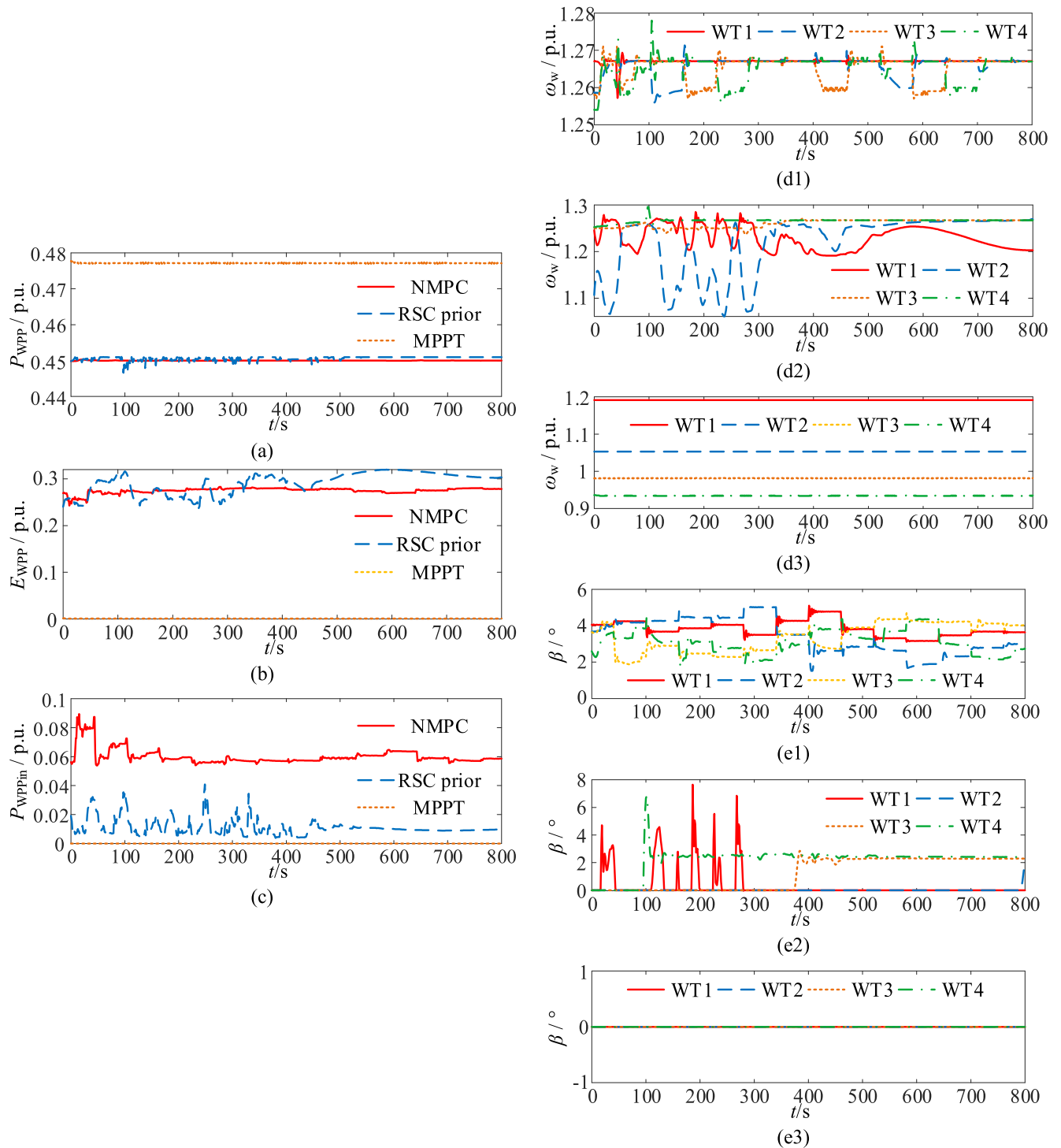


Fig. 11. Simulations of the WPP active power dispatch in constant wind scenario. (a) Active power of WPP, (b) Stored kinetic energy of WPP, (c) Increasable power of WPP, (d) rotor speeds of WTs with (d1) NMPC, (d2) RSC prior, (d3) MPPT strategies, (e) pitch angles of WTs with (e1) NMPC, (e2) RSC prior, (e3) MPPT strategies.

Table 1
Blade deflection of WTs.

Blade deflection	NMPC	RSC prior
WT1/deg	34.21	89.08
WT2/deg	33.35	2.09
WT3/deg	34.73	13.89
WT4/deg	41.39	31.74
Total/deg	143.68	136.8

The optimization problem can be solved within 10.072 s on a personal computer with an AMD Ryzen 7 4800H CPU. The sampling time is set to 1 minute, which is much larger than the computational time, ensuring the capability of the online application.

5.2.3. Turbulent wind with variable power reference

The wind scenario is the same as that in 5.2.2, but the power reference of WPP varies with wind speed every 1 min. The optimization approach without considering the time delay of wake effect, called Opt strategy, is applied in the proposed framework and compared in this

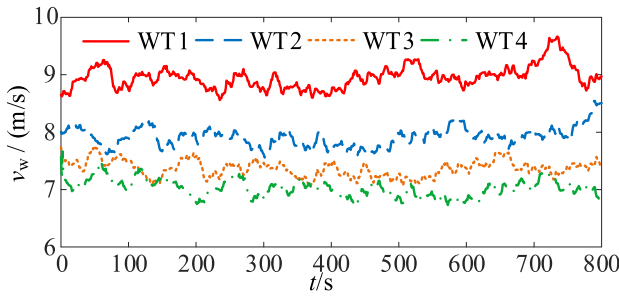


Fig. 12. Wind speed of each WT with MPPT strategy.

scenario. The results are shown in Fig. 14.

As can be seen in Fig. 14 (a), the active power output of WPP with NMPC strategy can track the reference value. The amount of stored kinetic energy of WPP with NMPC is larger than that with RSC prior strategy, shown in Fig. 14 (b). The increasable power of WPP is larger than that with RSC prior and Opt strategies during most of the time. As illustrated in Fig. 14 (c), the P_{WPPin} of WPP with NMPC has a violent fluctuation, because the calculation equations (7) and (10) are functions of P_{WPPin} on wind speeds of each WT, by which means the P_{WPPin} varies with wind speed. The mean values of P_{WPPin} every 60 s are also shown in Fig. 14 (c). Compared with the RSC prior and Opt strategies, the P_{WPPin} is respectively improved by 138.67 % and 39.62 % in average with the proposed strategy. It can be obtained that the WPP with the proposed strategy has a stronger temporary and sustained capabilities to support the frequency. The rotor speeds of each WT in the WPP are shown in Fig. 14 (d1) to (d3), which are with NMPC, RSC prior, Opt and MPPT strategies respectively.

6. Conclusion

The objective of this paper is to provide a reference for the operating status of each WT and prepare the WPP to participate in the frequency regulation. For this purpose, an active power dispatch strategy for the WPP based on the NMPC is proposed. By analyzing the difference of the output characteristics between a single WT and the whole WPP considering dynamic wake effect, the stored kinetic energy and increasable power of WPP are presented as the evaluation indicators of temporary and sustained APSCs of WPP. The WPP and WT controllers are coordinated in different timescales with the proposed bi-level framework. The operating statuses of WTs are optimized by the proposed NMPC strategy in WPP controller, and the coordinated active power control of WT is presented so that the WTs can adjust their operating statuses around the reference values provided by WPP controller to adapt to the fluctuations of wind sources.

Case studies show that the WPP's temporary and sustained APSCs are improved simultaneously by optimizing the operating statuses of WTs, without sacrificing blade deflection. Compared with the RSC prior method, the increasable power of WPP is improved by 104.88 % and 170.28 % in average with the proposed strategy in turbulent wind scenarios with constant power reference and variable power reference. Compared with the Opt strategy, the WPP's increasable power is increased by 39.62 % in turbulent wind scenario. Meanwhile, the stored kinetic energy in WPP is larger than that with traditional strategies in turbulent wind scenarios. Consequently, the effectiveness of the theoretical analysis and the superiority of the proposed strategy are validated. Finally, in order to describe the wake effect more precisely and to make the NMPC strategy applicable to the large-scale WPP, the modeling method of the dynamic wake effect and the computational efficiency of the algorithm will become our research focuses in future.

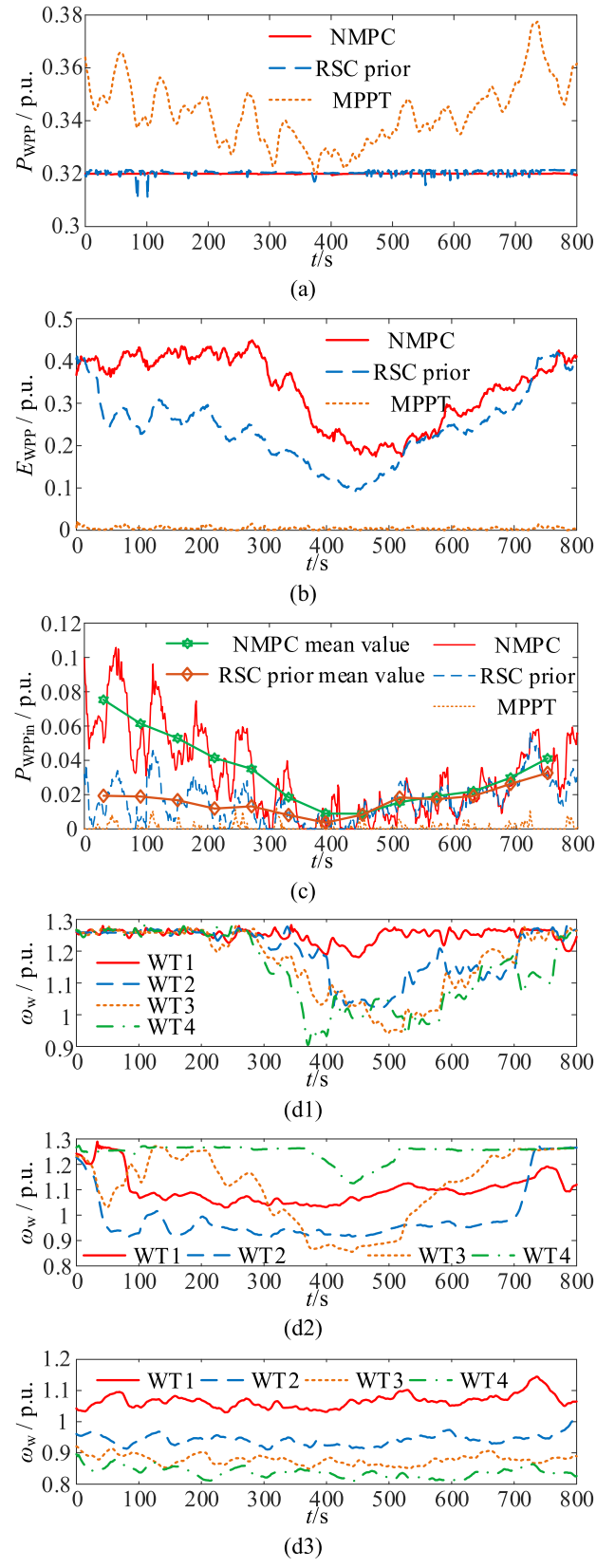


Fig. 13. Simulations of the WPP active power dispatch in turbulent wind and constant power reference scenario. (a) Active power of WPP, (b) Stored kinetic energy of WPP, (c) Increasable power of WPP, (d) rotor speeds of WTs with (d1) NMPC, (d2) RSC prior, (d3) MPPT strategies.

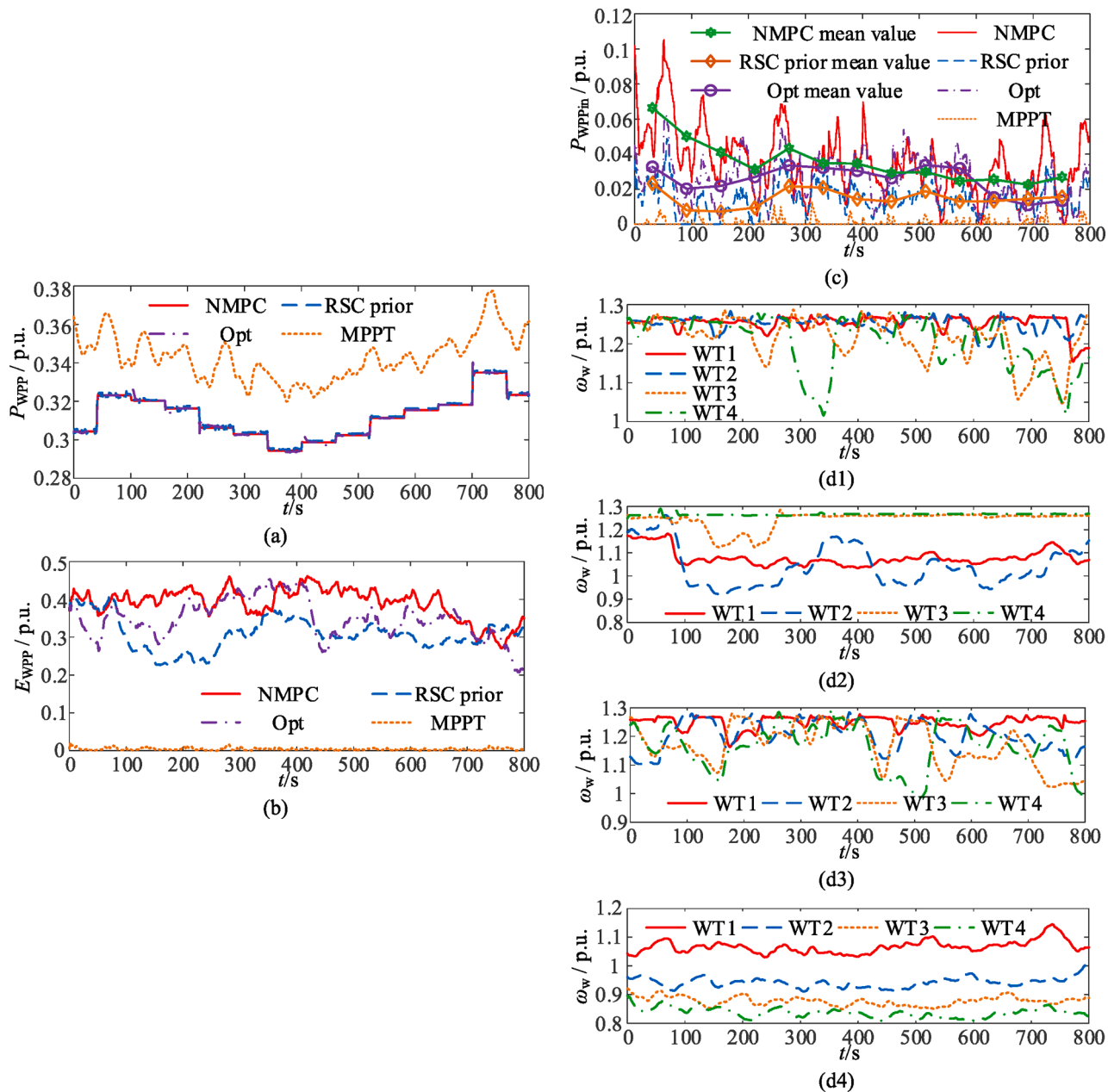


Fig. 14. Simulations of the WPP active power dispatch in turbulent wind and variable power reference scenario. (a) Active power of WPP, (b) Stored kinetic energy of WPP, (c) Increasable power of WPP, (d) rotor speeds of WTs with (d1) NMPC, (d2) RSC prior, (d3) Opt (d4) MPPT strategies.

CRediT authorship contribution statement

Zhengyang Hu: Conceptualization, Methodology, Software, Formal analysis, Writing – original draft, Writing – review & editing. **Bingtuan Gao:** Conceptualization, Supervision, Writing – review & editing. **Yongheng Mao:** Validation, Investigation, Writing – review & editing.

Declaration of Competing Interest

The authors declare that they have no known competing financial interests or personal relationships that could have appeared to influence the work reported in this paper.

Data availability

No data was used for the research described in the article.

Acknowledgement

This work was supported by the National Key Research and Development Program of China under Grant 2021YFB2400500.

References

- [1] Pan G, Gu W, Hu Q, Wang J, Teng F, Strbac G. Cost and low-carbon competitiveness of electrolytic hydrogen in China. *Energy Environ Sci* 2021;14: 4868–81.
- [2] Ye Y, Qiao Y, Lu Z. Revolution of frequency regulation in the converter-dominated power system. *Renew Sustain Energy Rev* 2019;111:145–56.
- [3] Choi S, Kang YC, Kim K, Lee Y, Terzija V. A frequency-responsive power-smoothing scheme of a doubly-fed induction generator for enhancing the energy-absorbing capability. *Int J Elec Power* 2021;131:107053.
- [4] Wang S, Tomsovic K. A Novel active power control framework for wind turbine generators to improve frequency response. *IEEE Trans Power Syst* 2018;33(6): 6579–89.
- [5] Fang J, Li H, Tang Y, Blaabjerg F. On the inertia of future more-electronics power systems, *IEEE. J Emerg Sel Top Power Electron* 2019;7(4):2130–46.

- [6] Lyu X, Jia Y, Liu T, Chai S. System-oriented power regulation scheme for wind farms: the quest for uncertainty management. *IEEE Trans Power Syst* 2021;36(5): 4259–69.
- [7] Dong Z, Li Z, Dong Y, Jiang S, Ding Z. Fully-Distributed Deloading Operation of DFIG-Based Wind Farm for Load Sharing. *IEEE Trans Sustain Energy* 2021;12(1): 430–40.
- [8] Ouyang J, Pang M, Li M, Zheng D, Tang T, Wang W. Frequency control method based on the dynamic deloading of DFIGs for power systems with high-proportion wind energy. *Int J Elec Power* 2021;128:106764.
- [9] Ramtharan G, Jenkins N, Ekanayake JB. Frequency support from doubly fed induction generator wind turbines. *IET Renew Power Gener* 2007;1(1):3.
- [10] Vidyanandan KV, Senroy N. Primary frequency regulation by deloaded wind turbines using variable droop. *IEEE Trans Power Syst* 2013;28(2):837–46.
- [11] Scholbrock A. Optimizing wind farm control strategies to minimize wake loss effects. M.S. thesis. Dept. Mech. Eng., Environ. Eng. Boulder, CO, USA: Univ. Colorado Boulder; 2011.
- [12] Xu Z, Chu B, Geng H, Nian X. Distributed Power Optimization of Large Wind Farms Using ADMM for Real-Time Control. *IEEE Trans Power Syst* 2022;37(6):4832–45.
- [13] Li Y, Xu Z, Zhang J, Yang H, Wong KP. Variable utilization-level scheme for load-sharing control of wind farm. *IEEE Trans Energy Convers* 2018;33(2):856–68.
- [14] Dong Z, Li Z, Dong Y, Jiang S, Ding Z. Fully-distributed deloading operation of WT-based wind farm for load sharing. *IEEE Trans Sustain Energy* 2021;12(1):430–40.
- [15] Gionfra N, Sandou G, Siguerdidjane H, Faillé D, Loevenbruck P. Wind farm distributed PSO-based control for constrained power generation maximization. *Renew Energy* 2019;133:103–17.
- [16] Ma S, Geng H, Yang G, Pal BC. Clustering-based coordinated control of large-scale wind farm for power system frequency support. *IEEE Trans Sustain Energy* 2018;9 (4):1555–64.
- [17] Lyu X, Jia Y, Xu Z. A novel control strategy for wind farm active power regulation considering wake interaction. *IEEE Trans Sustain Energy* 2020;11(2):618–28.
- [18] Ye L, Zhang C, Tang Y, Zhong W, Zhao Y, Lu P, et al. Hierarchical Model predictive control strategy based on dynamic active power dispatch for wind power cluster integration. *IEEE Trans Power Syst* 2019;34(6):4617–29.
- [19] Lin Z, Chen Z, Qu C, Guo Y, Liu J, Wu Q. A hierarchical clustering-based optimization strategy for active power dispatch of large-scale wind farm. *Int J Elec Power* 2020;121:106155.
- [20] Yao Q, Hu Y, Deng H, Luo Z, Liu J. Two-degree-of-freedom active power control of megawatt wind turbine considering fatigue load optimization. *Renew Energy* 2020;162:2096–112.
- [21] Yao Q, Hu Y, Zhao T, Guan Y, Luo Z, Liu J. Fatigue load suppression during active power control process in wind farm using dynamic-local-reference DMPC. *Renew Energy* 2022;183:423–34.
- [22] Lu P, Ye L, Zhao Y, Dai B, Tang Y. Review of meta-heuristic algorithms for wind power prediction: Methodologies, applications and challenge. *Appl Energy* 2021; 301:117446.
- [23] Würth I, Valdecabres L, Simon E, Möhrlein C, Uzunoglu B, Gilbert C, et al. Minut-scale forecasting of wind power—results from the collaborative workshop of IEA Wind task 32 and 36. *Renew Energy* 2019;12:712.
- [24] Valdecabres L, Peña A, Courtney M, Bremen L, Kühn M. Very short-term forecast of near-coastal flow using scanning lidars. *Wind energy science* 2018;3(1):313–27.
- [25] Zhen Z, Qiu G, Mei S, Wang F, Zhang X, Yin R, et al. An ultra-short-term wind speed forecasting model based on timescale recognition and dynamic adaptive modeling. *Int J Elec Power* 2022;135:107502.
- [26] Valdecabres L, Nygaard N, Vera-Tudela L, von Bremen L, Kühn M. On the use of dual-doppler radar measurements for very short-term wind power forecasts. *Remote Sens* 2018;10:1701.
- [27] Yang D, Kim J, Kang Y, Muljadi E, Zhang N, Hong J, et al. Temporary Frequency Support of a DFIG for High Wind Power Penetration. *IEEE Trans Power Syst* 2018; 33(3):3428–37.
- [28] Larsen GC, Madsen HA, Thomsen K, Larsen TJ. Wake meandering: A pragmatic approach. *Wind Energy* 2008;11:377–95.
- [29] Jensen N. A note on wind generator interaction. Risø National Laboratory, Tech. Rep. 1983.
- [30] Gao R, She X, Husain I, Huang AQ. Solid-state-transformer interfaced permanent magnet wind turbine distributed generation system with power management functions. *IEEE Trans Ind Appl* 2017;53(4):3849–61.
- [31] Gill S, Stephen B, Galloway S. Wind turbine condition assessment through power curve copula modeling. *IEEE Trans Sustain Energy* 2012;3(1):94–101.
- [32] Kheshti M, Ding L, Nayeripour M, Wang X, Terzija V. Active power support of wind turbines for grid frequency events using a reliable power reference scheme. *Renew Energy* 2019;139:1241–54.